

Modelling seasonal growth and composition of the kelp *Saccharina latissima*

Ole Jacob Broch · Dag Slagstad

Received: 12 October 2010 / Revised and Accepted: 8 June 2011 / Published online: 6 July 2011
© Springer Science+Business Media B.V. 2011

Abstract A dynamical model for simulating growth of the brown macroalga *Saccharina latissima* is described. In addition to wet and dry weights, the model simulates carbon and nitrogen reserves, with variable C/N ratio. In effect, the model can be used to emulate seasonal changes in growth and composition of the alga. Simulation results based on published, environmental field data are presented and compared with corresponding data on growth and composition. The model resolves seasonal growth, carbon and nitrogen content well, and may contribute to the understanding of how seasonal growth in *S. latissima* depends simultaneously on a combination of several environmental factors: light, nutrients, temperature and water motion. The model is applied to aquaculture problems such as estimating the nutrient scavenging potential of *S. latissima* and estimating the potential of this kelp species as a raw material for bioenergy production.

Keywords *Saccharina latissima* · Mathematical model · Seasonal growth · Reserve dynamics · Integrated multi-trophic aquaculture · Bioenergy

Introduction

An important aspect of the ecology of certain common kelps in the North Atlantic is their seasonal pattern of growth and storage of nutrients and polysaccharides. The kelp *Saccharina latissima* (L.) Lane, Mayes, Druel and Saunders (sugar kelp) stores nutrients in late winter and early spring, and utilise these nutrients for a prolonged period of growth through late spring into early summer. Growth is reduced in summer, when the plants store carbohydrates, stays low through autumn and increases again from about mid-winter, when stored carbohydrates are used for growth (Sjøtun 1993). Throughout the year, the chemical composition of *S. latissima* varies considerably (Haug and Jensen 1954; Sjøtun and Gunnarsson 1995).

Understanding this yearly cycle of growth and composition is important to obtain more precise estimates of net primary production and hence to obtain a better understanding of the ecological importance of *S. latissima*. For exploitation of this plant, both as a natural resource and for cultivation purposes, it is desirable to have as detailed knowledge as possible of the raw material.

In this paper, we present a dynamical model for the kelp *S. latissima*. The model includes nitrogen and carbon reserves, allowing us to simulate seasonal growth and changes in composition realistically. There has been renewed interest lately in *S. latissima* as a species for commercial aquaculture, as a species in integrated multi-trophic aquaculture and as a raw material for bioenergy (Sanderson 2009; Adams et al. 2009).

Bartsch et al. (2008) call for a more “holistic explanation” of growth performance of *Laminaria sensu lato* spp. (including, in this context, *S. latissima*), and the

This work was supported by the Norwegian Research Council project number 173527, “Integrated open seawater aquaculture, technology for sustainable culture of high productive areas”.

O. J. Broch (✉) · D. Slagstad
SINTEF Fisheries and Aquaculture,
7465 Trondheim, Norway
e-mail: ole.jacob.broch@sintef.no

present model may be regarded as a contribution to this. Our main purpose has been to develop a model that can be used to build an individual-based population model. The model is also useful within aquaculture as a tool for optimizing production strategies or production potential. In addition, we model carbohydrate content, making the model applicable to estimating the potential of *S. latissima* as a raw material in biofuel production. Examples of such applications are given in “Applications of the model”.

The paper is organized so that in “Model description”, we present the main equations of the model, the parameters are estimated in “Model parameters”, the model scenarios and the results from these are presented in “Simulations and results” and a discussion follows in “Discussion”.

Model description

A schematic overview of the model is presented in Fig. 1. A list of the main variables can be found in Table 1 while the main equations are presented in Table 2.

Variables and basic assumptions

The state variables of the model are frond area A (one side, projected area), nitrogen reserves N and carbon reserves C . Area A is measured in dm^2 , while N (resp. C) is measured in gN (resp. gC) per gram structural mass (sw). By structural mass, we mean the mass of the kelp frond minus the water and the nitrogen (N) and carbon (C) reserves. This is similar to the “DW” used

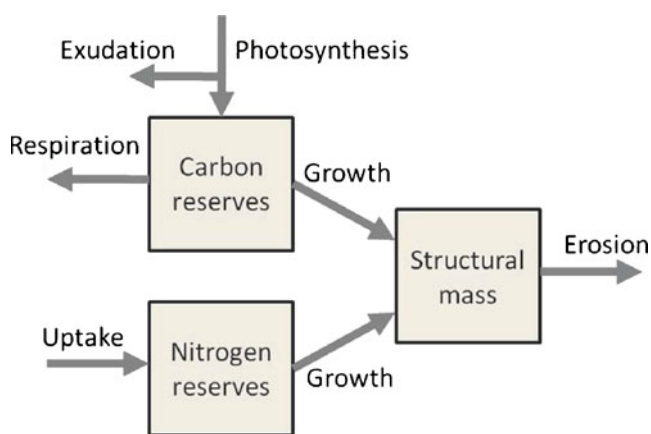


Fig. 1 Schematic overview of the model

by Schaffelke (1995). Note that we actually model only the kelp frond.

We use three derived variables to describe various aspects of the biomass: structural weight W_s , dry weight W_d (dw) and wet weight W_w (ww). See “Calculation of some important derived quantities”.

It is necessary to make a few, basic assumptions. Firstly, we assume that the structural mass and each reserve separately have fixed chemical compositions. This is called the assumption of *strong homeostasis* in DEB theory (Kooijman 2000). It does not mean that the chemical composition of the whole organism stays fixed. Instead, the composition of the kelp will depend on the relative abundance of the reserves. In particular, the C/N ratio will vary. Secondly, we assume that volume is proportional to A and that A is proportional to structural mass. It follows that the dry weight per area, as well as the water content, of the structural mass is always the same. The structural mass per area is denoted by k_A (see “Weight and area” below). Increasing or decreasing reserves will not affect the volume or area in the present model, but they may lead to varying density of the lamina (frond).

The environmental variables influencing growth and composition of the kelp in the present model are: temperature (T), irradiance (I), water current speed (U) and nutrient concentration (X) in the water. See Table 1 for the units used here. The exact effect of each of the four environmental factors on the growth and physiology of *S. latissima* will be described in detail in the next subsection. We will assume that salinity does not influence growth (although in reality it may—Gerard et al. 1987) due to lack of precise quantitative information (Bartsch et al. 2008). Neither will we consider general water turbidity here and wave exposure, although they may be as important for the nutrient uptake of some kelps as irradiance water current speed.

S. latissima has rather “flat” absorption and action spectra in the range 400–650 nm (Dring 1992), so we will use irradiance without taking into account the light’s spectral distribution.

Main equations

The main model equations, with a short description of their meaning, are listed in Table 2, while more detailed descriptions are provided next. Parameters are estimated in “Model parameters” and listed in Table 3. The differential Eqs. 1, 7 and 9 form the basis of the model.

Table 1 Model variables and calculated quantities

Symbol	Unit	Description
A	dm^2	Fronnd area, state variable
C	g C (g sw)^{-1}	Carbon reserves, relative to W_s , state variable
N	g N (g sw)^{-1}	Nitrogen reserve, relative to W_s , state variable
μ	day^{-1}	Specific growth rate (area), derived variable
W_w	g	Total wet weight of sporophyte, derived variable
W_d	g	Total dry weight, derived variable
W_s	g	Dry weight of structural mass, derived variable
β	$\text{g O}_2 \text{ dm}^{-2} \text{ h}^{-1} (\mu\text{mol photons m}^{-2} \text{ s}^{-1})^{-1}$	Photoinhibition parameter, auxiliary variable
P_S	$\text{g O}_2 \text{ dm}^{-2} \text{ h}^{-1}$	Photosynthesis parameter, auxiliary variable
I	$\mu\text{mol photons s}^{-1} \text{ m}^{-2}$	Irradiance (PAR), environmental variable
T	$^\circ\text{C}$	Water temperature, environmental variable
U	ms^{-1}	Water current speed, environmental variable
X	mmol L^{-1}	Substrate nutrient concentration, environmental variable

Growth and frond area

The rate of change with respect to time (t) of frond area A is assumed to satisfy the following differential equation:

$$\frac{dA}{dt} = [\mu(A, N, C, T, t) - \nu(A)]A. \tag{1}$$

The function μ should be thought of as a gross area specific instantaneous growth rate, while ν , described in detail in “Apical frond loss” below, determines the rate of frond loss. *S. latissima* experiences a continuous loss of apical tissue that may well result in a net loss of biomass in the summer to early winter (Sjötun 1993).

The gross growth rate μ is calculated based on Droop’s cell quota model (Droop 1983; Harrison and Hurd 2001). We treat the N and C reserves in the same way, and then use the minimum principle to calculate growth rates (Droop et al. 1982). We also take into consideration effects of temperature, size and photoperiod on growth. This leads to the following:

$$\begin{aligned} \mu(A, N, C, T, t) = & f_{\text{area}} f_{\text{temp}} f_{\text{photo}} \\ & \times \min\{1 - N_{\text{min}}/N, 1 - C_{\text{min}}/C\}. \end{aligned} \tag{2}$$

Here, N_{min} is the minimal reserve nutrient (nitrogen) level, while C_{min} is the minimal reserve carbon pool. The forcing functions f_{area} , f_{temp} and f_{photo} take into

Table 2 Model equations

Equation		Description
1	$dA/dt = (\mu - \nu)A$	Rate of change of frond area
2	$\mu = f_{\text{area}} f_{\text{photo}} f_{\text{temp}} \min\{1 - N_{\text{min}}/N, 1 - C_{\text{min}}/C\}$	Specific growth rate
3	$f_{\text{area}}(A) = m_1 \exp(-(A/A_0)^2) + m_2$	Effect of size on growth rate
4	$f_{\text{temp}}(T) = \begin{cases} 0.08T + 0.2 & \text{for } -1.8 \leq T < 10 \\ 1 & \text{for } 10 \leq T \leq 15 \\ 19/4 - T/4 & \text{for } 15 < T \leq 19 \\ 0 & \text{for } T > 19 \end{cases}$	Effect of temperature on growth rate
5	$f_{\text{photo}}(n) = a_1[1 + \text{sgn}(\lambda(n)) \lambda(n) ^{1/2}] + a_2$	Seasonal influence on growth rate
6	$\nu(A) = \frac{10^{-6} \exp(\epsilon A)}{(1 + 10^{-6}(\exp(\epsilon A) - 1))}$	Fronnd erosion
7	$dN/dt = k_A^{-1} J - \mu(N + N_{\text{struct}})$	Rate of change in nitrogen reserves
8	$J = J_{\text{max}} \frac{X}{K_X + X} \left(\frac{N_{\text{max}} - N}{N_{\text{max}} - N_{\text{min}}} \right) (1 - \exp(-U/U_{0.65}))$	Nitrate uptake rate
9	$dC/dt = k_A^{-1} [P(I, T)(1 - E(C)) - R(T)] - (C + C_{\text{struct}})\mu$	Rate of change in carbon reserves
10	$P(I, T) = P_S \left(1 - \exp\left(-\frac{\alpha I}{P_S}\right) \right) \exp\left(-\frac{\beta I}{P_S}\right)$	Gross photosynthesis
14	$R(T) = r_1 \exp\left(\frac{T_A}{T_1} - \frac{T}{T_1}\right)$	Temperature dependent respiration
15	$E(C) = 1 - \exp[\gamma(C_{\text{min}} - C)]$	Carbon exudation

Table 3 Parameters

Symbol	Value	Unit	Description
A_0	6	dm ²	Growth rate adjustment parameter
α	3.75×10^{-5}	$\text{g C dm}^{-2} \text{h}^{-1} (\mu\text{mol photons m}^{-2} \text{s}^{-1})^{-1}$	Photosynthetic efficiency
C_{\min}	0.01	g C (g sw)^{-1}	Minimal carbon reserve
C_{struct}	0.20	g C (g sw)^{-1}	Amount of carbon per unit dry weight of structural mass
γ	0.5	g C g^{-1}	Exudation parameter
ε	0.22	A^{-1}	Fronde erosion parameter
I_{sat}	200	$\mu\text{mol photons m}^{-2} \text{s}^{-1}$	Irradiance for maximal photosynthesis
J_{max}	1.4×10^{-4}	$\text{g N dm}^{-2} \text{h}^{-1}$	Maximal nitrate uptake rate
k_A	0.6	g dm^{-2}	Structural dry weight per unit area
k_{dw}	0.0785		Dry weight to wet weight ratio of structural mass
k_C	2.1213	g (g C)^{-1}	Mass of carbon reserves per gram carbon
k_N	2.72	g (g N)^{-1}	Mass of nitrogen reserves per gram nitrogen
m_1	0.1085		Growth rate adjustment parameter
m_2	0.03		Growth rate adjustment parameter
μ_{max}	0.18	day ⁻¹	Maximal area specific growth ratio
N_{\min}	0.01	g N (g sw)^{-1}	Minimal nitrogen reserve
N_{max}	0.022	g N (g sw)^{-1}	Maximal nitrogen reserve
N_{struct}	0.01	g N (g sw)^{-1}	Amount of nitrogen per unit dry weight of structural mass
P_1	1.22×10^{-3}	$\text{g C dm}^{-2} \text{h}^{-1}$	Maximal photosynthetic rate at $T = T_{P1}^\circ\text{K}$
P_2	1.44×10^{-3}	$\text{g C dm}^{-2} \text{h}^{-1}$	Maximal photosynthetic rate at $T = T_{P2}^\circ\text{K}$
a_1	0.85		Photoperiod parameter
a_2	0.3		Photoperiod parameter
R_1	2.785×10^{-4}	$\text{g C dm}^{-2} \text{h}^{-1}$	Respiration rate at $T = T_{R1}$
R_2	5.429×10^{-4}	$\text{g C dm}^{-2} \text{h}^{-1}$	Respiration rate at $T = T_{R2}$
T_{R1}	285	°K	Reference temperature for respiration
T_{R2}	290	°K	Reference temperature for respiration
T_{AP}	1,694.4	°K	Arrhenius temperature for photosynthesis
T_{APH}	25,924	°K	Arrhenius temperature for photosynthesis at high end of range
T_{APL}	27,774	°K	Arrhenius temperature for photosynthesis at low end of range
T_{AR}	11,033	°K	Arrhenius temperature for respiration
$U_{0.65}$	0.03	m s^{-1}	Current speed at which $J = 0.65J_{\text{max}}$
K_X	4	$\mu\text{mol L}^{-1}$	Nitrate uptake half saturation constant

account effects of size, temperature and time of the year, respectively, and will be described shortly (“Effect of size” to “Photoperiodic effect” below). The maximal theoretical growth rate, under ideal conditions when all the factors in Eq. 2 are maximized simultaneously, is denoted by μ_{max} .

Effect of size

We assume that the gross specific growth rate depends on the size of the plant and that smaller plants grow relatively faster than larger ones. There should be some limiting value (when the frond area is large) for the gross specific growth rate, while growth rates should stay high for frond areas close to 0. $\partial\mu/\partial A$ should be negative. A simple functional response with these properties is provided by the function:

$$f_{\text{area}}(A) = m_1 \exp[-(A/A_0)^2] + m_2, \quad (3)$$

where $m_2 = \lim_{A \rightarrow \infty} f_{\text{area}}$ and $m_1 + m_2 = f_{\text{area}}(0)$. A_0 determines at what area the specific growth rate will drop significantly.

In this way, small sporophytes will tend to grow relatively faster than larger ones.

Effect of temperature

The temperature influence is adapted from Petrell and Alie (1996) and Bolton and Lüning (1982)

$$f_{\text{temp}}(T) = \begin{cases} 0.08T + 0.2 & \text{for } -1.8 \leq T < 10 \\ 1 & \text{for } 10 \leq T \leq 15 \\ 19/4 - T/4 & \text{for } 15 < T \leq 19 \\ 0 & \text{for } T > 19 \end{cases} \quad (4)$$

Photoperiodic effect

According to Kain (1989) and Sjøtun (1995) *S. latissima* is a “season anticipator”, indicating that some external signal triggers changes in the growth pattern, rather

than e.g. reduced nutrient availability. The seasonal trigger is probably day length (Lüning 1993).

We let the *change* in day length force the growth rate μ as follows. Let $L(n)$ denote the length of Julian day number $n \bmod 365$ (366 for leap years). See e.g. Sakshaug et al. (2009) for a calculation of $L(n)$. Let $\Delta L(n) = L(n) - L(n - 1)$ denote the change in day length from day $n - 1$ to day n . Then $\Delta L(n) > 0$ whenever $-10 < n \leq 171$, $\Delta L(n) < 0$ for $172 \leq n < 355$ and $|\Delta L|$ is largest at the equinoxes. Normalizing the change in day length, we let $\lambda(n) = \Delta L(n) / \max_{1 \leq i \leq 365} \Delta L(i)$, so that $-1 \leq \lambda(n) \leq 1$. The photoperiodic influence on the growth rate at day number n is given by

$$f_{\text{photo}}(n) = a_1 [1 + \text{sgn}(\lambda(n))|\lambda(n)|^{1/2}] + a_2, \tag{5}$$

where the parameters a_1 and a_2 are chosen so that the maximal value of f_{photo} is 2 while sgn denotes the sign function. The effect of the f_{photo} -factor is to let the growth rate decrease whenever the day length decreases, and increase whenever the day length increases. Note that latitude is indirectly taken into account through photoperiodism.

Apical frond loss

S. latissima loses biomass continuously due to erosion of the frond (Sjøtun 1993). The two predominant factors forcing apical frond erosion seem to be age of tissue and water motion (Sjøtun 1993; Kawamata 2001; Buck and Buchholz 2005). However, Sjøtun (1993) found that longer laminae more easily eroded than shorter ones. In order to avoid keeping track of the exact age of each part of the frond we assume that erosion is taking place all the time, and that the relative amount of eroded tissue increases with increasing frond area and is “negligibly small” when the blade is “very small”. Thus v , the function describing the relative rate of frond loss, will depend on A . We let

$$v(A) = \left(\frac{10^{-6} \exp(\varepsilon A)}{(1 + 10^{-6}(\exp(\varepsilon A) - 1))} \right). \tag{6}$$

The number 10^{-6} says at what rate frond is lost when “ $A = 0$ ”, while ε is the rate at which erosion increases as A increases. One should not infer logistic growth or loss of the frond from Eq. 6. We shall not consider water movement effects on frond erosion here, as there is little quantitative information available.

Nitrogen reserves and nutrient uptake

The total amount of nitrogen in the organism is the sum of structural and reserve nitrogen. A fixed fraction of the structural mass is devoted to nitrogen, N_{struct} .

Reserve nitrogen is denoted by $N \text{ gN}(\text{gsw})^{-1}$. It is spent on growth of the structural mass. We assume that N has a minimal value N_{min} and a maximal value N_{max} . Thus, the total minimal nitrogen content, per unit structural mass, is given by $N_{\text{struct}} + N_{\text{min}}$. The dynamics are expressed by the differential equation

$$\frac{dN}{dt} = k_A^{-1} J - \mu (N + N_{\text{struct}}) \tag{7}$$

(Fig. 1). Here, J is the nutrient uptake rate per unit area:

$$J = J_{\text{max}} \left[1 - \exp\left(\frac{-U}{U_{0.65}}\right) \right] \left(\frac{N_{\text{max}} - N}{N_{\text{max}} - N_{\text{min}}} \right) \frac{X}{K_X + X}. \tag{8}$$

The rightmost factor is a Holling type II functional response (Holling 1959) (Michaelis–Menten uptake kinetics). X is the external nutrient concentration and K_X is the half saturation constant for N uptake. The factor in the middle takes into consideration internal nutrient reserve concentrations (Solidoro et al. 1997). Following Hurd et al. (1996), the leftmost factor takes into consideration water current speed on the uptake rate. $U_{0.65}$ is the current speed at which the uptake is 65% of the optimal one (Hurd et al. 1996). Finally, J_{max} is the maximal theoretical uptake rate under ideal conditions.

The nitrogen dynamics part of the model is consistent, in the sense that the kelp will never require more nitrogen for growth than there is available in the reserves, as long as the time step in the numerical calculation scheme is reasonably short.

Using the Droop equation (2) for macroalgae requires introducing an extra parameter, the “critical tissue N content” (Lobban and Harrison 1994; Harrison and Hurd 2001). The division of minimal N content into N_{min} and N_{struct} is one way of doing this. Furthermore, in the case when N is limiting, and whenever N is close to N_{min} , the response of μ to a change in N depends on the size of N_{min} .

Carbon reserves, photosynthesis and respiration

The total amount of carbon is the sum of structural and reserve carbon. The fraction of structural carbon to structural dry weight is denoted by C_{struct} . The unit for C is $\text{g C}(\text{gsw})^{-1}$, with a minimal value of C_{min} ; there is no maximal value. As for nitrogen, the minimal carbon content, per unit structural mass, is then $C_{\text{struct}} + C_{\text{min}}$.

The carbon dynamics are governed by the differential equation:

$$\frac{dC}{dt} = k_A^{-1} [P(I, T)(1 - E(C)) - R(T)] - \mu(C + C_{\text{struct}}), \quad (9)$$

(Fig. 1). The functions P and R describe gross photosynthesis and respiration, respectively. The exudation rate E combines exuded (actively excreted) and leaked carbohydrates. The significance of dividing structural carbon into C_{min} and C_{struct} is the same for carbon as for nitrogen.

Gross photosynthesis is calculated as

$$P(I, T) = P_S(T) \left[1 - \exp\left(-\frac{\alpha I}{P_S(T)}\right) \right] \exp\left(-\frac{\beta I}{P_S(T)}\right), \quad (10)$$

where I is irradiance ($\mu\text{mol photons m}^{-2} \text{s}^{-1}$) (Platt et al. 1980). The unit of P is $\text{g C dm}^{-2} \text{h}^{-1}$. The parameter α is estimated based on published values in “[Model parameters](#)”, while the relations between the other quantities in Eq. 10 are given by

$$P_S = \frac{\alpha I_{\text{sat}}}{\ln(1 + \alpha/\beta)}, \quad (11)$$

and

$$P_{\text{max}} = \frac{\alpha I_{\text{sat}}}{\ln(1 + \alpha/\beta)} \left(\frac{\alpha}{\alpha + \beta}\right) \left(\frac{\beta}{\alpha + \beta}\right)^{\beta/\alpha}, \quad (12)$$

(Platt et al. 1980). The maximal photosynthetic rate P_{max} is temperature dependent (Dring 1992) and is calculated according to an Arrhenius law (Kooijman 2000):

$$P_{\text{max}}(T) = \frac{P_1 \exp\left(\frac{T_{\text{AP}}}{T_{\text{P1}}} - \frac{T_{\text{AP}}}{T}\right)}{1 + \exp\left(\frac{T_{\text{APL}}}{T} - \frac{T_{\text{APL}}}{T_{\text{PL}}}\right) + \exp\left(\frac{T_{\text{APH}}}{T_{\text{PH}}} - \frac{T_{\text{APH}}}{T}\right)}. \quad (13)$$

In the above, P_1 is the maximal photosynthetic rate at a reference temperature T_{P1} . The parameters T_{AP} , T_{APL} , T_{APH} are all Arrhenius temperatures to be estimated in “[Photosynthesis and respiration](#)”. The Arrhenius temperatures are based on reference temperatures T_{PL} and T_{PH} at the extremes of the temperature range for photosynthesis. The unit used in Eq. 13 is $^{\circ}\text{K}$. P_{max} is achieved at an irradiance of $I = I_{\text{sat}}$, while photoinhibition occurs at irradiances higher than this. The parameter I_{sat} denotes the light intensity at which maximal photosynthesis is reached (Bartsch et al. 2008), and should not be confused with the *light saturation point* I_k .

The variable β , related to light inhibition, is calculated by solving Eq. 12 by Newton’s method (Adams 2007) using a start value of $\beta_0 = 1 \times 10^{-9}$ and ten iterations. Then β is used in Eq. 11 to calculate P_S , which is finally used in Eq. 10 to calculate the gross photosynthetic rate.

The rationale behind the correction factor (the denominator) in Eq. 13 is that chemical reactions increase with increasing temperatures (the numerator), but that there is an optimal temperature window for such reactions in living organisms. The optimal temperature range for growth in *S. latissima* seems to be 10–15 $^{\circ}\text{C}$ (Fortes and Lüning 1980; Bolton and Lüning 1982).

The complete photosynthate is assumed to go straight to the carbon reserves after exuded carbon has been deducted. Respired carbon is deducted from the reserves. The respiration rate is affected by temperature and obeys

$$R(T) = r_1 \exp\left(\frac{T_{\text{AR}}}{T_{\text{R1}}} - \frac{T_{\text{AR}}}{T}\right), \quad (14)$$

(Duarte and Ferreira 1997; Kooijman 2000). Here, r_1 denotes the respiration rate at the reference temperature T_{R1} , and T_{AR} is the Arrhenius temperature estimated from respiration rates at T_{R1} and T_{R2} K. See “[Photosynthesis and respiration](#)”. The respiration is assumed to include both activity and basal respiration, including what is required for growth and active nutrient uptake.

The exudation rate is governed by

$$E(C) = 1 - \exp[\gamma(C_{\text{min}} - C)]. \quad (15)$$

Exuded carbon is deducted directly from the photosynthate (Eq. 9). The parameter γ controls the rate at which carbohydrates are exuded. It is estimated in “[Model parameters](#)”. The function involved here should be monotonically increasing. Furthermore, since exponential type laws are involved in both photosynthesis and respiration, the choice of an exponential type functional response is appropriate.

Extreme carbon limitation

Since we have assumed that respiration takes place regardless of photosynthetic activity, the carbon reserve may in principle drop below the minimal level C_{min} . Because of Eq. 2 this is clearly unacceptable. In cases of extreme carbon limitation, we let the kelp lose structural mass while we keep $C = C_{\text{min}}$. The amount of frond area lost, A_{lost} , is calculated from the amount of structural carbon needed to retain $C = C_{\text{min}}$. If $C < C_{\text{min}}$,

the total carbon discrepancy is $k_A A(C_{\min} - C)$. We must have $A_{\text{lost}} k_A C_{\text{struct}} = k_A A(C_{\min} - C)$, so that

$$A_{\text{lost}} = A(C_{\min} - C) / C_{\text{struct}}.$$

Calculation of some important derived quantities

We next explain how to calculate the derived variables structural weight (W_s), dry weight (W_d) and wet weight (W_w).

The structural weight is defined to be equal to the total dry weight minus the weight of the surplus storage reserves and is proportional to frond area (“Main equations”):

$$W_s = k_A A,$$

where the parameter k_A is the amount of structural dry weight per area (“Weight and area”). The actual weights of the reserves are higher than the weights of just the carbon or nitrogen in them, because the C -reserves consist of carbohydrates, and the N -reserves may contain NO_3 (Sjøtun and Gunnarsson 1995). Thus, we have to introduce parameters k_C and k_N which denote the mass of surplus carbon and nitrogen reserves, respectively, per unit mass of carbon and nitrogen. The total dry weight is computed as

$$W_d = k_A [1 + k_N(N - N_{\min}) + N_{\min} + k_C(C - C_{\min}) + C_{\min}] A \tag{16}$$

The fraction of dry weight of the structural mass is denoted by k_{dw} (“Dry and wet weight”; Table 3). The reserves are assumed to contain no water. Hence, total wet weight W_w is given by

$$W_w = k_A [k_{\text{dw}}^{-1} + k_N(N - N_{\min}) + N_{\min} + k_C(C - C_{\min}) + C_{\min}] A \tag{17}$$

The total carbon and nitrogen contents are calculated as

$$C_{\text{total}} = (C + C_{\text{struct}}) W_s \tag{18}$$

and

$$N_{\text{total}} = (N + N_{\text{struct}}) W_s, \tag{19}$$

respectively.

It follows from the last two equations and Eq. 10 that there is a lower, but no upper, bound for the C/N ratio in the model. Because of the structure and morphology of kelps, a certain amount of carbon is required and usually more than in microalgae (Atkinson and Smith 1983; Baird and Middleton 2004).

We are also interested in the total amount of carbon fixed and frond area produced by a kelp plant. From

$t = t_1$ to $t = t_2$ the total net carbon fixed and the total gross frond area produced is given by

$$\int_{t_1}^{t_2} W_s C' dt, \quad \int_{t_1}^{t_2} \mu A dt,$$

respectively. A plot of seasonal gross area production is presented in Fig. 3a, b.

Model implementation and numerics

The model was implemented in Matlab and Fortran 90. Approximations to the solutions of the differential equations were computed by a standard Euler method (Iserles 1996).

Model parameters

Parameter values are summarized in Table 3.

Weight and area

We use weight per area ratios to compute biomasses. Values from Gerard (1988) range from about 0.18 to 0.61 g dw dm⁻². Ahn et al. (1998) found a per dm² dry weight of 1.35 g. We obtain values of 0.89–1.46 g dw dm⁻² by subtracting the laminaran and mannitol from the g dw dm⁻² figures in Lüning (1979). Based on the above figures, we choose the value $k_A = 0.6$ g sw dm⁻² for structural mass per area. Actual dry weight per area may be much greater.

Nutrient uptake

The nitrate uptake half saturation constant is set to $K_X = 4$. There are not much data available for uptake half saturation constants for *S. latissima*. Espinoza and Chapman (1983) found nitrate half saturation constants for NO_3 uptake in *Saccharina longicuris*, which is the same species (McDevit and Saunders 2010), varying from 4.4 to 6.3 (at 9°C). Half saturation constants for growth lie in the range 1.4–2.9 (Chapman et al. 1978; Espinoza and Chapman 1983).

Values for maximal nitrate uptake rates for *S. latissima* vary a lot throughout the literature. Subandar et al. (1993) report a maximal NO_3 uptake rate of about 10.4 $\mu\text{mol g dw}^{-1} \text{h}^{-1}$, while Ahn et al. (1998) have mean uptake rates ranging from 4.6 to 10.6 $\mu\text{mol g dw}^{-1} \text{h}^{-1}$. Bartsch et al. (2008) give values of 13.6–14.6 $\mu\text{mol g dw}^{-1} \text{h}^{-1}$.

We use uptake rates per unit projected frond area. The mathematical statement of the N -dynamics in terms of dry weight would be more awkward. We

choose the value $10 \mu\text{mol g dm}^{-2} \text{h}^{-1}$, leading to $J_{\text{max}} = 1.4 \times 10^{-4} \text{ g N dm}^{-2} \text{h}^{-1}$ in Eq. 8.

Hurd et al. (1996) found values for $U_{0.65}$ in *Macrocystis integrifolia* to be around 0.05 m s^{-1} . Although a different species, fronds of *S. latissima* have morphological similarities to those of *M. integrifolia*. We decide on the value $U_{0.65} = 0.03 \text{ m s}^{-1}$ (Stevens et al. 2003).

Photosynthesis and respiration

Various photosynthetic rates for *S. latissima* may be found in Bartsch et al. (2008). Because we use frond area A as a state variable, we will base our parameters on information about area specific photosynthetic activity. Lüning (1979, 1990) found net maximal (P_{max}) rates of about $2 \text{ m l O}_2 \text{ dm}^{-2} \text{h}^{-1}$ at a water temperature of 12°C for *S. latissima* sporophytes grown at 2–4.5 m depth. Gerard (1988) got a maximal gross rate of about $1.1959 \mu\text{mol O}_2 \text{ cm}^{-2} \text{h}^{-1}$ (average of values for kelps from four different light acclimation levels) at 15°C for kelps from a “shallow” (5 m) habitat. Adding dark respiration rates from Lüning (1979) at 4.5 m and 12°C we get gross maximal photosynthesis rates of $3.5986 \times 10^{-3} \text{ g O}_2 \text{ dm}^{-2}$ (Lüning 1979) and $3.8269 \times 10^{-3} \text{ g O}_2 \text{ dm}^{-2}$ (Gerard 1988). Converting to gC and using a photosynthetic quotient of $\text{PQ} = 1.105$ (Gerard 1988), we arrive at a maximal photosynthetic rate of $P_1 = 1.22 \times 10^{-3} \text{ g C dm}^{-2} \text{h}^{-1}$ at $T = T_{P_1} = 285^\circ\text{K}$ (Lüning 1979) and $P_2 = 1.30 \times 10^{-3} \text{ g C dm}^{-2} \text{h}^{-1}$ at $T = T_{P_2} = 288^\circ\text{K}$ (Gerard 1988). Using these rates and temperatures, we calculate the Arrhenius temperature for photosynthesis from the numerator in Eq. 13 as follows

$$T_{\text{AP}} = ((T_{P_1})^{-1} - (T_{P_2})^{-1})^{-1} \ln(P_2/P_1) = 1,694.4^\circ\text{K}.$$

All temperatures need to be expressed as $^\circ\text{K}$ here. The low and high extreme temperatures for photosynthesis are assumed, somewhat arbitrarily, to be $T_{\text{PL}} = 271^\circ\text{K}$ and $T_{\text{PH}} = 296^\circ\text{K}$. The corresponding rates are further assumed to be $3.394 \times 10^{-4} \text{ g C dm}^{-2} \text{h}^{-1}$ and $6.787 \times 10^{-4} \text{ g C dm}^{-2} \text{h}^{-1}$, respectively. According to Davison (1987) rates are reduced significantly at the extremes of the temperature range. We obtain $T_{\text{APL}} = 27,774^\circ\text{K}$ and $T_{\text{APH}} = 25,924^\circ\text{K}$.

A maximal photosynthetic rate P_{max} is assumed to be achieved at an irradiance of $I = I_{\text{sat}} = 200 \mu\text{mol photons m}^{-2} \text{s}^{-1}$, for all temperatures. Photo-inhibition occurs at irradiances higher than I_{sat} . The average of the values recorded in Bartsch et al. (2008) is 215, but the values vary considerably.

We choose a photosynthetic efficiency of $\alpha = 3.75 \times 10^{-5} \text{ g C dm}^{-2} \text{h}^{-1} (\mu\text{mol photons m}^{-2} \text{s}^{-1})^{-1}$, which is a

bit higher than what we would get from Lüning (1979, 1990).

In order to check the consistency of the data, we calculate the photosynthetic rate at $T = 12^\circ\text{C}$ using the values of P_1 , I_{sat} and α just chosen in Eqs. 10 and 13. We obtain a gross photosynthetic rate of $P \approx 2.95 \times 10^{-4} \text{ g C dm}^{-2} \text{h}^{-1}$, at $I = 10 \mu\text{mol photons m}^{-2} \text{s}^{-1}$, which is just slightly higher than corresponding, independent measurements of about $2.87 \times 10^{-4} \text{ g C dm}^{-2} \text{h}^{-1}$ (Lüning and Dring 1985).

A respiration rate of $R_1 = 2.785 \times 10^{-4} \text{ g C dm}^{-2} \text{h}^{-1}$ at $T_{R_1} = 285$ was taken from Lüning (1979). We choose $R_2 = 5.429 \times 10^{-4} \text{ g C dm}^{-2} \text{h}^{-1}$ at $T_{R_2} = 290^\circ\text{K}$, a bit higher than Lüning’s value at that same temperature. The Arrhenius temperature T_{AR} for respiration in *S. latissima* was then calculated from these data using Eq. 14 as $T_{AR} = (T_{R_1}^{-1} - T_{R_2}^{-1})^{-1} \ln(R_2/R_1) = 41,940^\circ\text{K}$.

Because A represents projected area, it is taken into account that the dark side of the frond is also contributing to photosynthesis and respiration, as in Lüning (1979).

The exudation parameter is set to $\gamma = 0.5$. There are no good exudation rates available. Duarte and Ferreira (1993) use a figure of 20% of the net annual photosynthate for *Gelidium sesquipedale*. Other very general figures vary from 0.02 to 40% (Lobban and Harrison 1994; Mann 2000). Our parameter has been chosen by tuning the model to field observations (“Simulations and results”).

Composition and sizes of structural mass and reserves

Next we estimate the factors k_C and k_N introduced in “Calculation of some important derived quantities”. Each of the reserves and the structural mass will be represented by so-called generalized compounds (Kooijman 2000).

The two most important storage carbohydrates in *S. latissima* are mannitol and laminaran (Bartsch et al. 2008). The combined laminaran and mannitol content of the fronds of *S. latissima* varies from about 5 to 45% of the dry weight (Black 1950; Haug and Jensen 1954). We will treat these carbohydrates as belonging to the reserves only. Alginate will be assumed to be part of the structural mass, but 10% (in molar amounts) of the reserves will contribute to the alginate as well. This is to accommodate for sufficient flexibility in the alginate content and to be sure that the combined amount of mannitol and laminaran does not get too large. Thus, the carbon reserves consist, in molar amounts, of 70% mannitol and laminaran and 10% of alginate. The remaining 20% is simply stored as carbon. The

stoichiometric formulas for mannitol, laminaran and alginate are assumed to be $C_6H_{14}O_6$, $C_{150}H_{252}O_{126}$ and $C_{132}H_{178}O_{133}$, respectively. Thus, 1 g C corresponds to 2.5278 g mannitol, 2.26 g laminaran and 2.4558 g alginate, respectively. If we assume that mannitol and laminaran exist in equal molar amounts, we have that 1 g C corresponds to

$$k_C = 0.7 \cdot (2.5278 + 2.26)/2 + 0.1 \cdot 2.4558 + 0.2 \cdot 1 = 2.1213 \text{ g reserves.}$$

We assume that half of the surplus reserve nitrogen $N - N_{\min}$ is stored as nitrogen and half of it as nitrate (NO_3). Thus 1 g N corresponds to

$$k_N = 0.5 \cdot (1 + 4.432) = 2.72 \text{ g reserves.}$$

In order to compute the sizes of the reserves, we note that the nitrogen content lies in the range from 0.7 to about 4.5% dw (Chapman et al. 1978; Sjøtun 1993). Carbon content lies in the range 19–38% dw (Sjøtun 1993; Bartsch et al. 2008). We choose the values $N_{\min} = 0.01$, $N_{\max} = 0.022$, $N_{\text{struct}} = 0.01$, $C_{\min} = 0.01$ and $C_{\text{struct}} = 0.2$. Cf. Eqs. 19, 18 and 16.

The alginate content of *S. latissima* fronds has been reported to lie in the range 11–32% dw^{-1} (Black 1950; Haug and Jensen 1954). We let the alginate account for 30% of the structural dry weight. An additional 10% of the C reserves are also added to the alginate.

To summarize, reserve carbohydrate and alginate content, expressed as fractions of dry weight, are computed as

$$\text{Carbohydrates} = [0.7 \cdot 2.3939 \cdot (C - C_{\min})]/W_d,$$

and

$$\text{Alginate} = [0.3W_s + 0.1 \cdot 2.4558 \cdot (C - C_{\min})]/W_d,$$

respectively. See Fig. 4a for simulated seasonal carbohydrate and alginate content. Note that the choice of $k_C = 2.1213$ means that the carbon content can never exceed about 47% dw^{-1} .

Dry and wet weight

Some published figures for dry matter content lie in the range 8–26% (Black 1950). In our model, the fraction k_{dw} of dry weight in the structural mass is fixed. Because it is the variation in storage carbohydrates that seems to account for most of the variation in dry matter content (Black 1950), we assume that $W_d/W_w = 0.08$ when $N = N_{\max} = 0.022$ and $C = C_{\min} = 0.011$. Using these data in the fraction W_d/W_w (see Eqs. 16 and 17), along with the values for k_N and k_C established in the previous section, we get $k_{dw} = 0.0785$. Thus, the

structural mass has a dry matter content of 7.48%. The absolute (theoretical) minimal dry matter content is 7.99%. Figure 7b displays simulated dry matter content.

Photoperiod

Though lamina growth in *S. latissima* is much reduced in Autumn, it is not zero even if there is a net loss of frond (Sjøtun 1993; Sjøtun and Gunnarsson 1995). Thus the growth factor f_{photo} is never set to zero either. We choose the values $a_1 = 0.85$ and $a_2 = 0.3$ in Eq. 5 so that we have $f_{\text{photo}} = 0.85[1 + \text{sgn}(\lambda(n))|\lambda(n)|^{1/2}] + 0.3$, with $0.3 \leq f_{\text{photo}} \leq 2$.

Growth rate and frond erosion

Published figures for growth rates for *S. latissima* vary a lot (Fortes and Lüning 1980; Bolton and Lüning 1982; Gerard et al. 1987; Sjøtun 1993; Sjøtun and Gunnarsson 1995; Sanderson 2009). Since the highest recorded growth rate that we have been able to find in the literature is a specific growth rate of about 0.18 day^{-1} (Chapman et al. 1978), a specific growth rate of 0.18 will be assumed under ideal environmental conditions, when reserves are maximized, at the right time of the year and when the plant is very small. We let $\mu_{\max} = 0.18$ and the maximal gross specific growth rate at “infinite” A equal 0.039. Because $\max_n(f_{\text{photo}}(n)) = 2$, $\max_T(f_{\text{temp}}) = 1$ and $\max_N(1 - N_{\min}/N) = 0.65$ (see Eq. 2), this means that we must set $m_2 = 0.039/(2 \cdot 0.65) = 0.03$ in Eq. 3. The number 0.039 was decided upon by comparing model results with growth data from Sjøtun (1993), but see also Gerard (1987). To have $\mu_{\max} = 0.18$, $m_1 + m_2 = 0.18/(2 \cdot 0.65) = 0.1385$, so that $m_1 = 0.1085$. $A_0 = 6$ in Eq. 3, by model adjustment.

The frond erosion parameter is chosen as $\varepsilon = 0.22A^{-1}$.

Simulations and results

Comparing model results with ecological data

Environmental data and ecological model

Although a lot of published material relates growth in *S. latissima* to at least one environmental factor (Lüning 1979; Gagné et al. 1982; Gerard 1988; Bartsch et al. 2008), we have not been able to find any complete datasets where growth and composition are recorded alongside monitoring the four environmental variables

used in our model. Light intensity is rarely recorded satisfactorily. The most complete dataset for our purposes is presented in Sjøtun (1993). In Sjøtun (1993), growth in length and width of the lamina are recorded for a full year, as well as carbon and nitrogen content. Water NO_3 concentration and temperature are recorded. In Sjøtun (1993), only temperatures from January to August 1982 are presented. Since the biological data, as well as the nutrient data, were collected from August 1981 to August 1982, we have included temperatures (<10 m depth) from approximately the same area from the International Council for the Exploration of the Sea (ICES, www.ices.dk) for the period August 1981–January 1982. See Fig. 2a. We have chosen data points from Sjøtun (1993) somewhat arbitrarily. The growth model is not very sensitive to temperature changes.

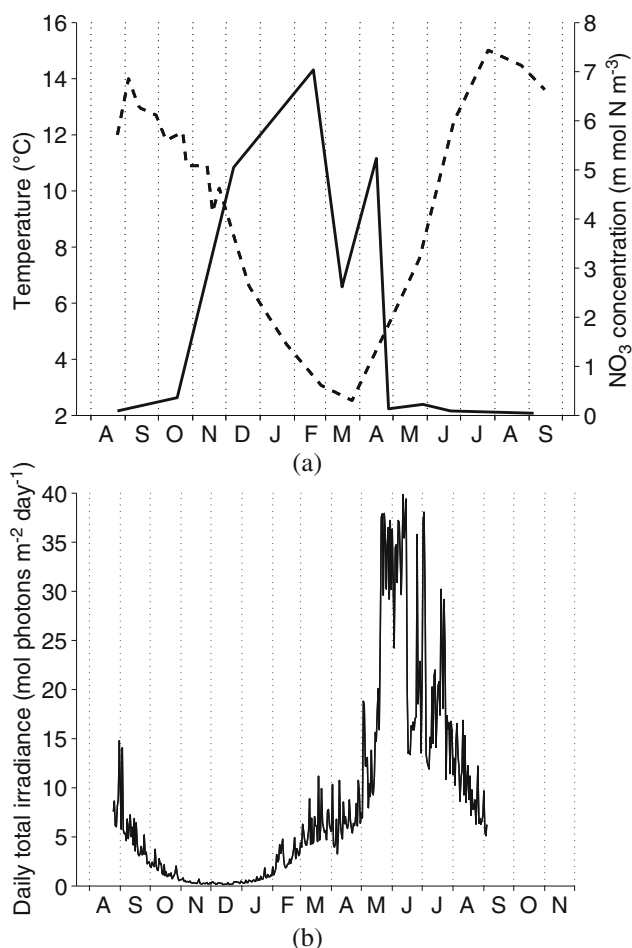


Fig. 2 Environmental data used to compare the model with published growth records. **a** NO_3 concentration ($\mu\text{mol NO}_3 \text{ L}^{-1}$) from Sjøtun (1993) (solid line) and temperature data from Sjøtun (1993) and ICES (www.ices.dk) (dashed line). **b** Simulated total daily irradiance at 5 m depth

In order to obtain realistic light data to test the model, we used a 1D version of the SINMOD 3D hydrodynamic, ecological and biochemical model system (Wassmann et al. 2006). The data in Sjøtun (1993) were collected in a fjord on the west coast of Norway, latitude $60^\circ 15' 24''$ N, longitude $5^\circ 11' 42''$ E. Data from SINMOD simulations with a 20-km horizontal resolution for the relevant area and time were used to force the 1D model. In the 1D model, light intensity depends on atmospheric conditions, depth, the density of phytoplankton (simulated in the ecological model) and on the (background) attenuation coefficient. At total of 46 vertical layers were used, with high resolution near the surface (0.5 m thickness) and thicker layers further down. The total depth was 295 m. Irradiance was calculated in the middle of each vertical cell. Thus seasonal and depth variations in the light attenuation for the relevant location and time (the years 1981–1982) are taken into consideration (Fig. 2b). The samples in Sjøtun (1993) were collected at 5 m below ELWS. Current speed data from SINMOD 3D was also used, chosen rather arbitrarily, taking into account tides. The average current speed in these data was 0.15 m s^{-1} .

The SINMOD 1D model also provides nitrate and temperature data. These data were used in the simulations in “Applications of the model” below (Fig. 5a, b).

Model results

Using the temperature and nutrient data in Fig. 2a, the light data in Fig. 2b and a time step of $\Delta t = 1 \text{ h}$, the model was run with the initial conditions $A(0) = 30 \text{ dm}^2$, $C(0) = 0.6$ and $N(0) = 0.01$. The environmental data from Sjøtun (1993) were linearly interpolated to accommodate for the 1 h time step. “Background” attenuation was set to 0.07 m^{-1} .

The modelled gross total frond area produced was about 131.4 dm^2 (dashed line Fig. 3a). The ratio of gross total produced frond area to “standing” frond area at the end of the simulation is about 3.67. In Fig. 3b averaged daily frond area grown is plotted. Data for length growth and width of *S. latissima* fronds from Sjøtun (1993) have been used to estimate the daily frond area grown. Seasonal variations are apparent. The average daily frond area produced is about 0.35 dm^2 . Carbon and nitrogen content, expressed as fractions of dry weight, are plotted in Fig. 3c, d, respectively.

In Fig. 4a, we have plotted reserve carbohydrate and alginate content from the same simulation. Note how the alginate and reserve carbohydrate levels vary according to “reciprocal” seasonal patterns.

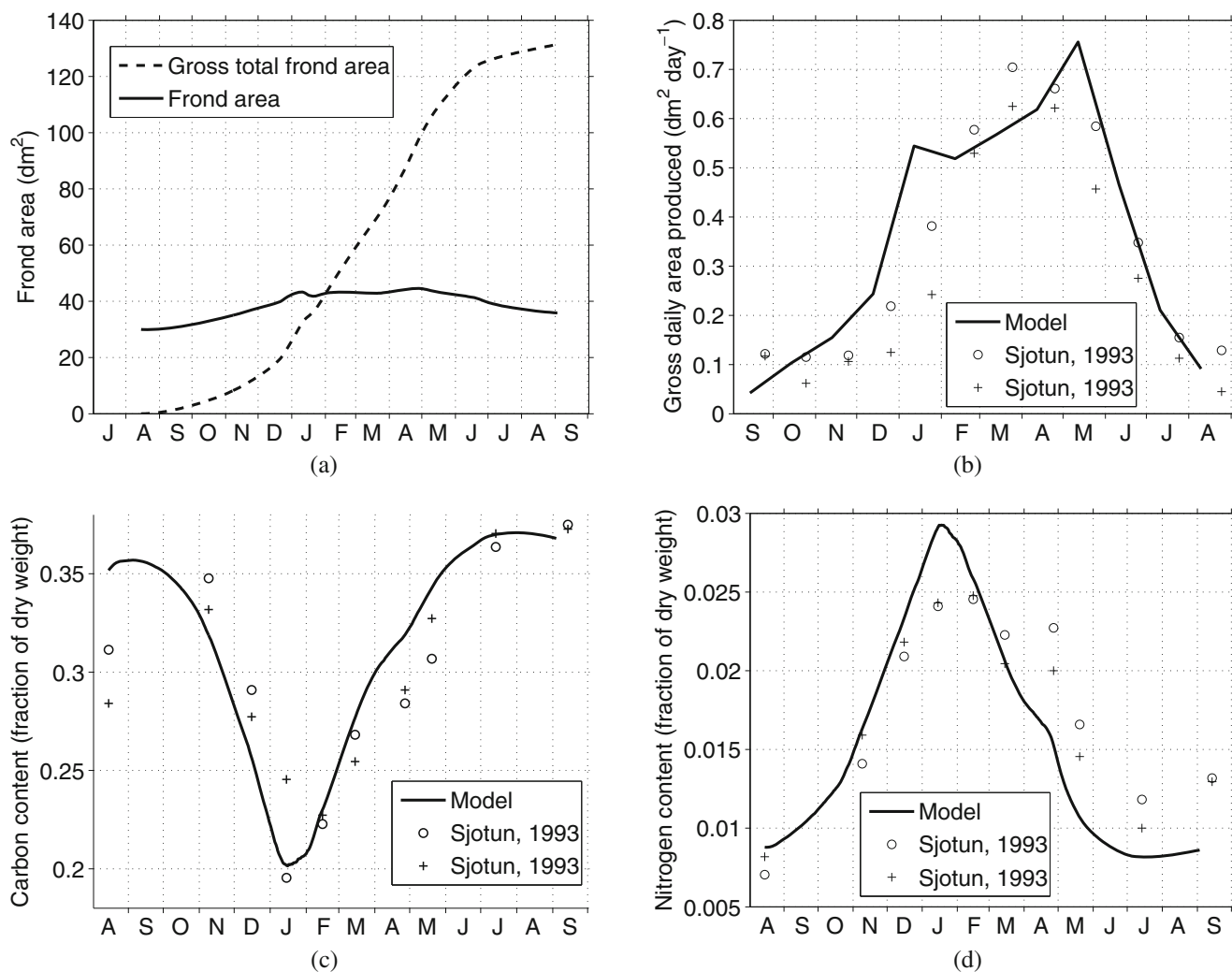


Fig. 3 **a** The *solid line* represents simulated standing frond area and the *dashed line* the simulated gross area produced. **b** Gross daily frond area produced. *Solid line*, averages of the daily area produced for the previous 30 days. *Circles*, daily area produced estimated from Sjøtun (1993) 2-year plants. *Crosses*, daily area produced estimated from Sjøtun (1993), 3-year plants.

c Carbon content expressed as fraction of dry weight. *Solid line*, model results. *Circles*, Sjøtun (1993) proximal/meristematic tissue. *Crosses*, apical frond tissue. **d** Nitrogen content expressed as fraction dry weight. *Solid line*, model results. *Circles* (o), Sjøtun (1993), 2-year plants. *Crosses*, Sjøtun (1993) 3-year plants

A simulated daily carbon budget for a kelp plant is set up in Fig. 4b. The budget runs over 385 days. The total amount of carbon fixed through photosynthesis the first 365 days is 125 g, of which 51 g is released through respiration. Of the remaining 74 g, 29 g is exuded as dissolved organic carbon (DOC). Thus, 39% of the fixed carbon is released in the process of exudation.

Applications of the model

In the following applications, data from the 1D ecological model were used (Fig. 5a, b). Water current speed

was set to 0.06 m s^{-1} and the “background” attenuation coefficient was 0.07 m^{-1} . The initial values $A(0) = 0.1$, $C(0) = 0.3$ and $N(0) = 0.022$ and a time step of $\Delta t = 0.5 \text{ h}$ were used.

Ecology: compensation depth

In this model run, the simulation period was 1 year (from January 12 until January 11). The light compensation depth (Fig. 6a) was determined as follows. Whenever the difference $P - R$ (see Eq. 9) was positive in depth layer k ($1 \leq k \leq 46$) and negative in layer

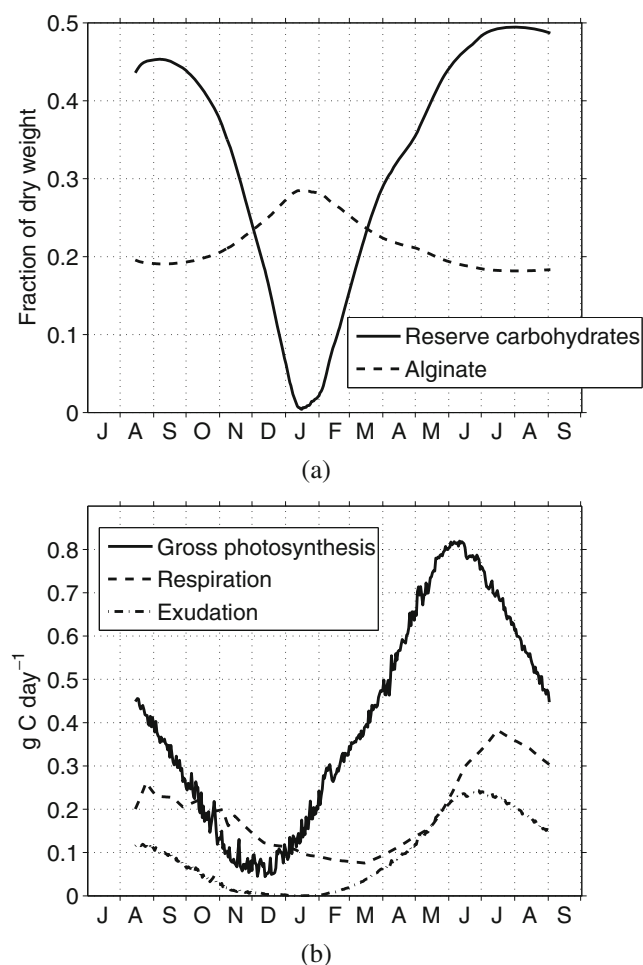


Fig. 4 Simulated carbohydrate content and carbon budget. **a** Reserve carbohydrate (solid line) and alginate (dashed line) content. **b** Simulated yearly carbon budget for a single kelp plant. Solid line, gross photosynthesis; dashed line, respiration; dash-dot line, exudation

$k + 1$, the boundary between layer k and layer $k + 1$ was set as the compensation depth. If $P - R$ were negative for all layers, the compensation depth was set to 0.

We see that the compensation depth is 0 from early November until early January, indicating a net carbon loss in this period but not necessarily zero growth. At times (later half of February; later half of May and in July–August), the light compensation depth is greater than the lower depth limit for the distribution of *S. latissima*, which is at least 25 m (Sundene 1953). The compensation depth is 20 m or less in the period of supposed fastest growth (April), indicating that below 20 m little carbon is accumulated (Fig. 6b) throughout the year. At 19.5 m depth the maximal total carbon content is 1.9 g, and at 30 m it is 0.07 g. At 5 and 10 m depth, the maximal carbon content is about 11.1 g and 7.8 g, respectively.

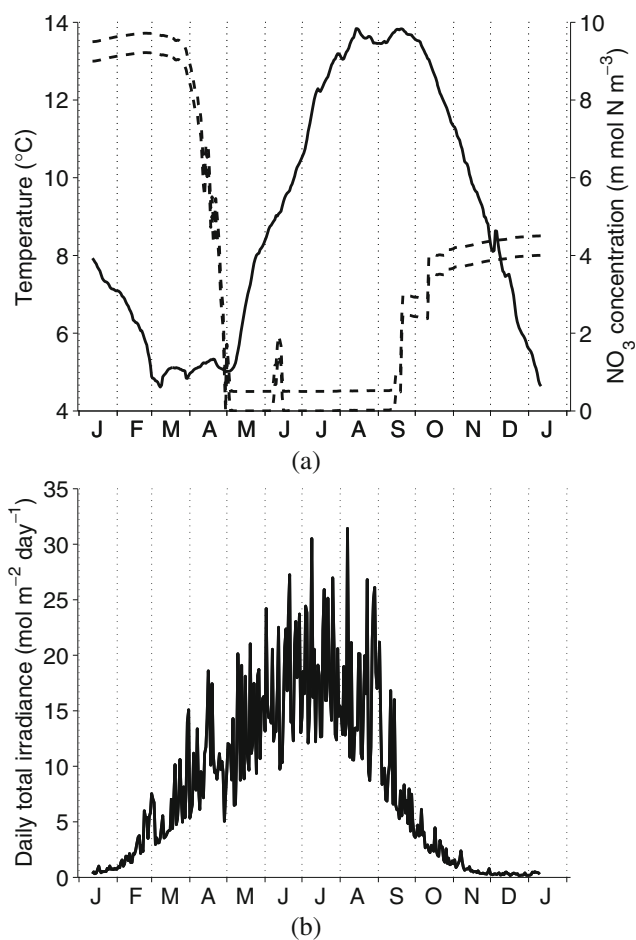


Fig. 5 **a** Simulated NO_3 (dashed lines) and temperature. The upper dashed line represents simulations with NO_3 concentration increased by $0.5 \mu\text{mol L}^{-1}$. **b** Simulated total daily irradiance at 3 m

Sugar kelp as bioremediator and integrated multi-trophic aquaculture

There is presently great interest in *S. latissima* as a bioremediator (Sanderson 2009). Integrated multi-trophic aquaculture aims at reducing environmental effects of, e.g. fish farming, at the same time increasing seaweed crops (Troell et al. 2009). We now study the nitrogen scavenging potential of *S. latissima* in rope cultures. We assume a cultivation period of 120 days from February 11 to June 11. The model indicates that mid-February is about the optimal time for plant out with a cultivation period ranging from 90 to 150 days. We get a period of fast growth and plentiful nutrients followed by a period when naturally occurring nutrients (NO_3) are scarce but irradiance levels generally high.

Using the environmental data provided by the 1D ecological model described above (Fig. 5a, b), the model was run with and without an added $0.5 \mu\text{mol N L}^{-1}$,

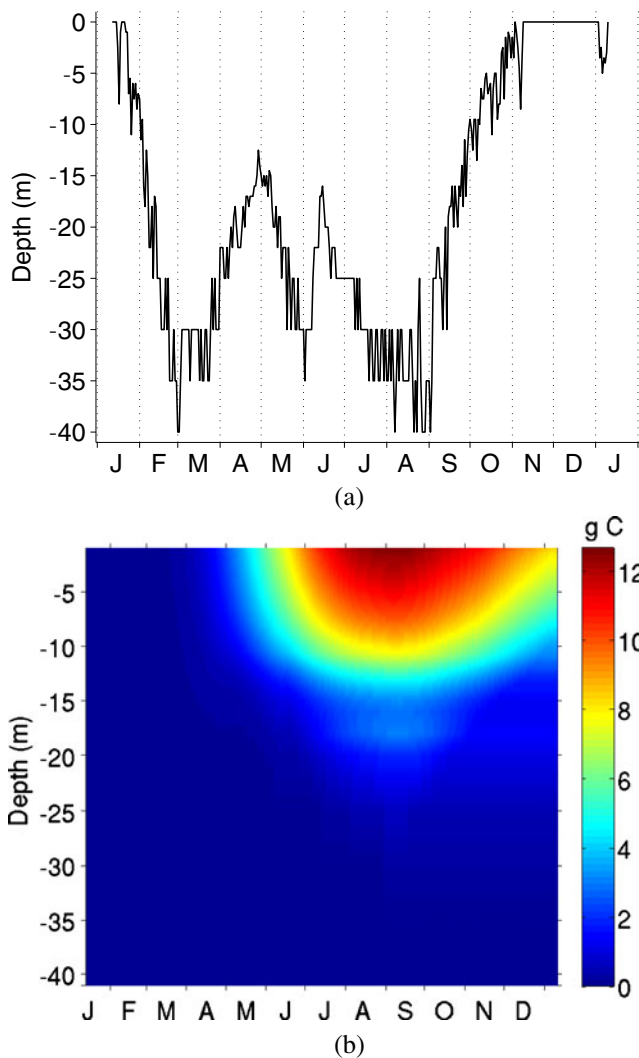


Fig. 6 **a** Compensation depth. **b** Absolute carbon content as a function of time and depth

an increase that might result from, e.g. Atlantic salmon (*Salmo salar*) farming (Sanderson 2009). The extra nutrients were made available to the kelp only, and not added to the overall nitrogen budget in the 1D model. We did not distinguish between NH_4 and NO_3 N.

In addition to the light attenuation in the 1D ecological model (“Comparing model results with ecological data”), denoted by k_{eco} , we also include self shading by the kelps, k_{kelp} , in the present scenario and the next (“Sugar kelp as a raw material for bioenergy”). Thus, the total attenuation is given by

$$k = k_{\text{eco}} + k_{\text{kelp}},$$

where k_{eco} is calculated as in Wassmann et al. (2006). The kelp light extinction depends on the number of kelp individuals per meter rope culture (n), the number

of vertically hanging ropes per m^{-2} (D), the fraction of incident light absorbed by the kelp fronds at any depth (a_{kelp}) and the area of kelp fronds (A):

$$k_{\text{kelp}} = -\log(1 - a_{\text{kelp}}(1 - (1 - AD)^n)).$$

The formula for k_{kelp} is inspired by that in Jackson (1987), but we assume that all kelp blades are ordered from the top downwards and take into consideration all layers of blades (Jackson stops after 2). Then the formula for the sum of a finite geometric series and the Lambert–Beer law are invoked. We use the values $a_{\text{kelp}} = 0.7$ (Jackson 1987), $n = 120$ and $D = 0.1$ (one vertical rope per 10 m^2).

Although growth of non-fertilized plants continue throughout the whole simulation period, growth slows down from the end of April onwards (Fig. 7a) both at 1 and 3 m. Fertilization sustains a high growth rate for the whole period at both depths and increases the final wet weight by about 43 (resp. 45%) at 1 (resp. 3 m). A conspicuous feature at both depths is the difference in dry matter content with and without fertilization (Fig. 7b).

In Fig. 7c, we have plotted the nitrogen scavenging potential (in g N (m rope)^{-1}) of one vertical kelp rope as a function of the total length of the rope (solid line) for the entire 120-day simulation period. The scenario with an added $0.5 \mu\text{mol N L}^{-1}$ was used. The dashed line in Fig. 7c indicates the number of ropes needed to scavenge 1 kg N from the environment during the 120-day period as a function of rope length.

A fish farm producing 1,000 tons of Atlantic salmon in 1 year releases about 44 tons of nitrogen to the environment in various forms, about two thirds of which is available for uptake by micro- and macroalgae (Olsen et al. 2008). Assuming that a farm producing 1,000 tons in 1 year releases 10 tons of N in the 120-day simulation period, we would need more than 80,000 ropes of 5 m length, covering an area of about 80 ha, to remove this amount of nitrogen in the present scenario.

Sugar kelp as a raw material for bioenergy

S. latissima is presently being considered as a raw material for energy production (Adams et al. 2009). Using the same simulation as in the previous subsection (120 days from February 11 to June 11), and assuming an ethanol yield of 0.583 L per kg glucose equivalents, we have calculated the ethanol yield by a single vertical *S. latissima* rope of 5-m total length, with and without exploiting the alginate, as a function of harvest date (Fig. 7d). When alginate is not included, only the storage polysaccharides are assumed to be used in the

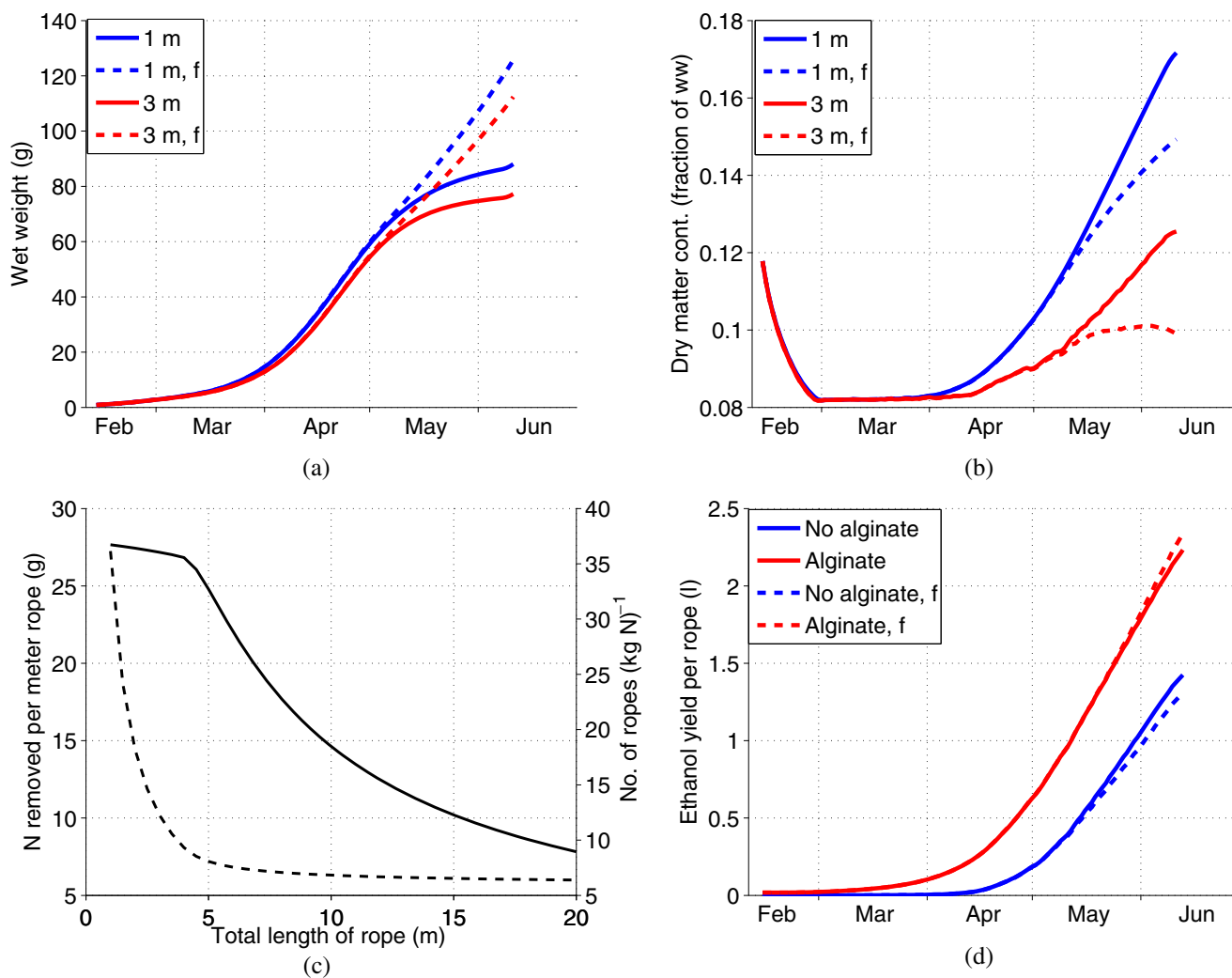


Fig. 7 **a** Simulated fresh weight of single *S. latissima* plants at 1 m (blue lines) and 3 m (red lines). Dashed lines, fertilized plants. **b** Dry matter content, expressed as fraction of fresh weight. **c** Nitrogen scavenging potential after 120 days as functions of the length of vertically hanging ropes. Solid line, g N removed per

meter rope. Dashed line, number of ropes needed to remove 1 kg N. **d** Ethanol yields from 5 m long vertical *S. latissima* ropes. Blue lines: alginate not used in the fermentation; red lines, alginate used in the fermentation. Solid lines, no fertilization; dashed lines, fertilization

fermentation. A density of 120 individuals m^{-1} was assumed, with a vertical rope density of one vertical rope per 10 m^2 . The effect of fertilization ($0.5 \mu\text{mol N L}^{-1}$) is indicated (dashed line). When the alginate is not used for fermentation the ethanol yield of the fertil-

ized plants does not surpass that of the unfertilized ones (lower two curves in Fig. 7d). When the alginate is included, yields are always greater when fertilizing (upper two curves). Fertilization leads to a decrease in the ethanol yield of almost 8% from 1.42 L by the end

Table 4 Sensitivity to selected parameters of the three states *A*, *N* and *C* after 120 days in the scenario in “Sugar kelp as bioremediator and integrated multi-trophic aquaculture”

Variable	Parameter									
	a_2	m_2	A_0	ε	γ					
<i>A</i>	-0.08	-0.46	-0.05	0.19	0.56	0.44	-0.08	0.08	-0.09	0.06
<i>N</i>	-0.02	0	-0.05	-0.02	-0.03	-0.01	0	0	-0.02	0
<i>C</i>	-0.07	0.10	-0.07	0.08	-0.10	0.07	-0.07	0.07	-0.34	-0.13

Parameters were perturbed $-/+ 50\%$ (left/right value in each column) ($\Delta p/p = \pm 0.5$) from the standard value

Table 5 Sensitivity to initial conditions of the three states *A*, *N* and *C* after 120 days in the scenario in “Sugar kelp as bioremediator and integrated multi-trophic aquaculture”

Variable	Initial condition				
	A(0)		C(0)		N(0)
<i>A</i>	0.75	0.46	0.18	0.23	−0.05
<i>N</i>	0.03	0.03	0	0.02	0
<i>C</i>	0	0	−0.09	0.08	−0.08

Initial conditions were perturbed −/+ 50% (left/right value in each column) ($\Delta p/p = \pm 0.5$) from the standard value, except *N*(0) perturbed only −50% from standard value of *N*(0) = 0.022

of the simulation when alginate is not fermented and an increase of more than 5% from 2.23 L to 2.35 L when alginate is fermented.

Sensitivity analyses

The sensitivity of a state variable (*x*) with respect to changes (Δp) in a parameter or initial condition (*p*) can be defined as

$$S = \frac{\Delta x/x}{\Delta p/p}, \tag{20}$$

(Jørgensen and Bendoricchio 2001, p. 27), where Δx is the change in *x* corresponding to the change in *p*. In our case *x* = *A*, *N* or *C* after 120 days in the scenario in “Sugar kelp as bioremediator and integrated multi-trophic aquaculture” (Tables 4 and 5). We test only those parameters that are not directly derived from corresponding parameters in the literature, and we test the initial values. We see from Tables 4 and 5 that $|S| < 1$ in all cases tested, which means that uncertainties in parameters and initial conditions are not amplified in the values of the state variables.

Discussion

Model mechanics

Although we have taken into account what are probably the most important variables to estimating kelp growth, uptake and production, we have also made a number of simplifications.

We have not considered frond morphology. There is evidence that blade morphology in Laminariales may not influence nitrogen uptake (Hurd et al. 1996), and that even if, e.g. current velocity may have an effect on blade morphology in *S. latissima*, the streamlining does not necessarily affect productivity (Gerard 1987). As for the possible effects of age, size and water movement on the rate of erosion of kelp fronds, there is little

data available, although Kawamata (2001) and Buck and Buchholz (2005) have looked into, e.g. adaption of algae to various flow regimes. In Sjøtun (1993), it is indicated that erosion in itself is not necessarily related to a fixed age, and we have used size rather than age to force erosion; Eq. 6.

The model describes seasonal variation in nitrogen and carbon content (Fig. 3c, d) reasonably well. The figures for leakage and exudation of photosynthates are somewhat controversial, ranging from about 1% to 40% (Lobban and Harrison 1994). Without exudation, carbon content in the model would be too high. Photosynthetic rates used in the model are not too high, however, since Lüning (1979) measured photosynthetic rates in August, when both carbohydrate content and photosynthetic rates were high. Some of the photosynthate, about 8%, should probably be exported to the stipe rather than be exuded (Hatcher et al. 1977). Reproduction and spore release is probably of minor importance in terms of carbon invested (Joska and Bolton 1987).

Future improvements to our model should thus include a more detailed model for photosynthesis and carbohydrate and protein synthesis, as well as a more mechanistic approach to nutrient uptake. A better description of frond erosion should also be attempted. We have made no distinction between newly formed tissue and old tissue, although the differences can be considerable (Sjøtun 1993; Sjøtun and Gunnarsson 1995; Bartsch et al. 2008), but this might be included as well, for instance by dividing the frond into meristematic and apical zones.

As for seasonal growth patterns, it is a question whether *S. latissima* has a low growth rate in summer/early autumn because nutrient concentrations are low or because of an endogeneous rhythm or photoperiodic forcing Eq. 5. There is evidence that day length forces the growth rate, but this has not been proved (Bartsch et al. 2008). Geographic and genetic variations may also be important. In Canada, growth rates in *S. longicuris* seem to be controlled by the seasonal variations in nutrient concentration rather than day length (Gagné et al. 1982). In Germany, growth in *S. latissima* was slow from July onwards, although nitrate concentrations were in the range 4–20 $\mu\text{mol L}^{-1}$ (Lüning 1979). It is interesting that growth in *S. latissima* seems to be at a maximum in March–April, while it is at a minimum in September, according to some investigations (Brinkhuis et al. 1984; Sjøtun 1993). Both extrema seem to occur when the changes in day length are at a maximum or minimum (resp.). Besides, reproduction seems to be timed, approximately, with the Autumn equinox. This is the reason why we have chosen to use the rate

of change of day length, and not day length itself, in the photoperiodic forcing function (Eq. 5). In some other kelps like *Laminaria hyperborea* and *Laminaria digitata*, the seasonal growth pattern is controlled by day length (Schaffelke and Lüning 1994), and growth stops in summer. However, *first-year L. hyperborea* sporophytes continue growing through summer (Sjøtun et al. 1996), and there is a possibility that the same pattern holds for *S. latissima*. If so, this would make *S. latissima* even more efficient as a bioremediator.

No biotic factors have been taken explicitly into account, although they are important (Lüning 1990). They are probably implicit in the choice of parameters.

Model verification

The results from “[Simulations and results](#)” indicate that the model resolves seasonal growth and composition well when the right environmental data are used as input (Fig. 2). As we have not had access to complete datasets for all environmental variables (irradiance is missing) as well as growth and composition data, we cannot do a full model validation.

Comparison with other models

The level of detail at which to pitch a model depends on its purpose. The aim of our present model has been to simulate seasonal growth of *S. latissima* individuals realistically, and to include enough details about variations in the composition. This has been accomplished through the inclusion of the C and N reserves. Some previous models for kelp (*S. latissima* and *S. japonica*) in aquaculture assume that light is not limiting, since cultivation depth may be varied (Petrell et al. 1993; Duarte et al. 2003). For investigating the aquaculture potential and ecology of *S. latissima* in high latitude environments (such as Norway and the Arctic) with distinct seasonal variations in light conditions, the inclusion of light dependency is crucial.

Cell quota models have been used in macroalgal models before, e.g. Solidoro et al. (1997) and Martins et al. (2007). However, we believe ours is the first dynamical growth model for *S. latissima* and similar species including both carbon and nutrient storage. In addition we have explicitly included aspects of seasonality (f_{photo}). The model may be useful in studying such phenomena in more detail.

Most recent macroalgal growth models have been part of quite complex ecological model systems, where the macroalgae have been included on a population level, e.g. Duarte et al. (2003), Trancoso et al. (2005) and Aveytua-Alcázar et al. (2008). We have focused

more on size and composition of individual plants in the present paper. The model has been included in a 1D ecological model, and may directly be used as part of a 3D model as well.

Applications

The results in “[Ecology: compensation depth](#)” indicate that, depending on water quality, a *S. latissima* population may not be very productive at depths below 20 m. Water clarity is explicitly taken into account through the attenuation coefficient. The great light compensation depth in February can be explained as the combined effect of low temperatures, and hence low respiration rates, and very low phytoplankton concentrations at this time. Although the simulated light compensation depth may be too great at times, our results for total carbon accumulation are logical, and show that *S. latissima* will mainly thrive above about 15 m. This is in line with Rueness and Fredriksen (1991). From an ecological perspective, our model results indicate that kelps have to compete not only for nutrients but also for light in the season of fast growth, and that phytoplankton may, indirectly, be one of the major competitors because in the 1D model they contribute to increasing the attenuation.

The results from the aquaculture applications in “[Applications of the model](#)” are reasonable. There is evidence that fertilization by cultivating kelps nearby fish farms may increase biomass yields significantly (Sanderson 2009). The model results also show how the effects of fertilization may depend on the timing. Whenever natural nutrients are plentiful (Fig. 6a), fertilization has little effect, but from early May onwards, growth is much increased by adding even quite low, albeit realistic (Sanderson 2009), levels of N (Fig. 7a).

The influence of fertilization by fish farm effluents on the composition (Fig. 7b, c) of macroalgae has been observed in practice (Martinez and Buschmann 1996); this is the so-called Neish effect (Neish et al. 1977). Most of the variation in dry matter content in *S. latissima* is caused by the storage and use of reserve carbohydrates (Black 1950). When N is limiting, fertilization will lead to increased growth, so that more of the C reserves is spent, and hence (relatively) less is accumulated in the reserves.

Our results (Fig. 7b, d) suggest that for bioenergy purposes fertilization of *S. latissima* plants may not necessarily be very effective, and even undesirable, because higher water content may lead to more demanding and costly pre-treatment, and the relative amount of waste matter will be greater, while the ethanol yield

is not much increased, or is even decreased if the structural polysaccharides are not included.

With a view towards bioremediation, our results suggest that little is gained by using vertical cultivation ropes longer than 4–5 m (Fig. 7c). The simulation results also indicate that the amount of *S. latissima* biomass needed to remove the full effluent from a salmon farm producing 1,000 tons a year is potentially vast. Abreu et al. (2009) present calculations that indicate that a 100 ha *Gracilaria chilensis* farm may be needed to bioremediate a farm producing 1,000 tons of salmon a year. Our figure of 80 ha (“[Sugar kelp as bioremediator and integrated multi-trophic aquaculture](#)”) compares well with this. This raises the questions of whether full bioremediation by kelp cultivation is actually feasible, and whether very large kelp cultures might have some negative impacts in terms of dissolved and particulate matter eroded from the fronds.

In reality, an effluent from salmon farming will vary with tides, currents, feeding intensity of the salmon etc. A simplified model of such a situation is described in Petrell et al. (1993) and Petrell and Alie (1996), but in order to provide precise estimates for the nitrogen scavenging potential of a large scale *S. latissima* farm, one will have to develop a detailed population model taking in account nutrient depletion and flow reduction in the farm. We will do so in a future paper, invoking the potential of the fully coupled 3D hydrodynamic and ecological model system SINMOD (Wassmann et al. 2006), of which only a one dimensional version was used here.

Acknowledgements The authors wish to thank K. Sjøtun for information about sampling dates and K. Sjøtun and Walter de Gruyter GmbH for granting permission to replot the data in Figs. 2a and 3b–d. They also thank M.O. Alver, M.J. Dring, I.H. Ellingsen, S. Forbord, K.I. Reitan and T. Størseth for valuable discussions and comments on the model and earlier versions of the manuscript. Two anonymous referees contributed several remarks that helped in improving the paper.

References

- Abreu H, Varela DA, Henríquez L, Villaroel A, Yarish C, Sousa-Pinto I, Buschmann AH (2009) Traditional vs. integrated aquaculture of *Gracilaria chilensis* C. In: Bird J, McLachlan J, Oliveira EC (eds) Productivity and physiological performance. *Aquaculture* 293:211–220
- Adams JM, Gallagher JA, Donnison IA (2009) Fermentation study on *Saccharina latissima* for bioethanol production considering variable pre-treatments. *J Appl Phycol* 21:569–574
- Adams RA (2007) *Calculus: a complete course*. Pearson Education, Paris
- Ahn O, Petrell RJ, Harrison PJ (1998) Ammonium and nitrate uptake by *Laminaria saccharina* and *Nereocystis luetkeana* originating from a salmon sea cage farm. *J Appl Phycol* 10:333–340
- Atkinson MJ, Smith SV (1983) C:N:P ratios of benthic marine plants. *Limnol Oceanogr* 28:568–574
- Aveytua-Alcázar L, Camacho-Ibar VF, Souza AL, Allen JI, Torres R (2008) Modelling *Zoostera marina* and *Ulva* spp. in a coastal lagoon. *Ecol Model* 218:354–366
- Baird ME, Middleton JH (2004) On relating physical limits to the carbon: nitrogen ratio of unicellular algae and benthic plants. *J Mar Syst* 49:169–175
- Bartsch I, Wiencke C, Bischof K, Buchholz CM, Buck BH, Eggert A, Feuerpfeil P, Hanelt D, Jacobsen S, Karez R, Karsten U, Molis M, Roleda MY, Schubert H, Schumann R, Valentin K, Weinberger F, Wiese J (2008) The genus *Laminaria sensu lato*: recent insights and developments. *Eur J Phycol* 43:1–86
- Black WAP (1950) The seasonal variation in weight and chemical composition of the common British Laminariaceae. *J Mar Biol Ass UK* 19:45–72
- Bolton JJ, Lüning K (1982) Optimal growth and maximal survival temperatures of Atlantic *Laminaria* species (phaeophyta) in culture. *Mar Biol* 66:89–94
- Brinkhuis BH, Mariani EC, Breda VA, Brady-Campbell MM (1984) Cultivation of *Laminaria saccharina* in the New York Marine Biomass Program. *Hydrobiologia* 116/117:266–271
- Buck BH, Buchholz CM (2005) Response of offshore cultivated *Laminaria saccharina* to hydrodynamic forcing in the North Sea. *Aquaculture* 250:674–691
- Chapman ARO, Markham JW, Lüning K (1978) Effects of nitrate concentration on the growth and physiology of *Laminaria saccharina* (phaeophyta) in culture. *J Phycol* 14:195–198
- Davison IR (1987) Adaptation of photosynthesis in *Laminaria saccharina* (phaeophyta) to changes in growth temperature. *J Phycol* 23:273–283
- Dring MJ (1992) *The biology of marine plants*. Cambridge University Press, Cambridge
- Droop MR (1983) 25 years of algal growth kinetics—a personal view. *Bot Mar* 26:99–112
- Droop MR, Mickleson JM, Scott JM, Turner MF (1982) Light and nutrient status of algal cells. *J Mar Biol Ass UK* 62:403–434
- Duarte P, Ferreira JG (1993) A methodology for parameter estimation in seaweed productivity modelling. *Hydrobiologia* 260/261:183–189
- Duarte P, Ferreira JG (1997) A model for the simulation of macroalgal population dynamics and productivity. *Ecol Model* 98:199–214
- Duarte P, Meneses R, Hawkins AJS, Zhu M, Fang J, Grant J (2003) Mathematical modelling to assess the carrying capacity for multi-species culture within coastal waters. *Ecol Model* 168:109–143
- Espinoza J, Chapman ARO (1983) Ecotypic differentiation of *Laminaria longicurvis* in relation to seawater nitrate concentration. *Mar Biol* 74:213–218
- Fortes MD, Lüning K (1980) Growth rates of North Sea macroalgae in relation to temperature, irradiance and photoperiod. *Helgol Wiss Meeresunters* 34:15–29
- Gagné JJ, Mann KH, Chapman ARO (1982) Seasonal patterns of growth and storage in *Laminaria longicurvis* in relation to differing patterns of availability of nitrogen in the water. *Mar Biol* 69:91–101
- Gerard V (1988) Ecotypic differentiation in light-related traits of the kelp *Laminaria saccharina*. *Mar Biol* 97:25–36
- Gerard VA (1987) Hydrodynamic streamlining of *Laminaria saccharina* Lamour. In response to mechanical stress. *J Exp Mar Biol Ecol* 107:237–244

- Gerard VA, DuBois K, Greene R (1987) Growth responses of two *Laminaria saccharina* populations to environmental variation. *Hydrobiologia* 151/152:229–232
- Harrison PJ, Hurd CL (2001) Nutrient physiology of seaweeds: application of concepts to aquaculture. *Cah Biol Mar* 42:71–82
- Hatcher BG, Chapman ARO, Mann KH (1977) An annual carbon budget for the kelp *Laminaria longicuris*. *Mar Biol* 44:85–96
- Haug A, Jensen A (1954) Seasonal variations in the chemical composition of *Alaria esculenta*, *Laminaria saccharina*, *Laminaria hyperborea* and *Laminaria digitata* from Northern Norway. Tech. Rep. 4, Norwegian Institute of Seaweed Research
- Holling CS (1959) Some characteristics of simple types of predation and parasitism. *Can Entomol* 91:385–398
- Hurd CL, Harrison PJ, Druehl LD (1996) Effect of seawater velocity on inorganic nitrogen uptake by morphologically distinct forms of *Macrocystis integrifolia* from wave-sheltered and exposed sites. *Mar Biol* 126:205–214
- Iserles A (1996) A first course in the numerical analysis of differential equations. Cambridge University Press, Cambridge
- Jackson GA (1987) Modelling the growth and harvest yield of the giant kelp *Macrocystis pyrifera*. *Mar Biol* 95:611–624
- Jørgensen SE, Bendoricchio G (2001) Fundamentals of ecological modelling, 3rd edn. Elsevier, Amsterdam
- Joska MAP, Bolton JJ (1987) In situ measurement of zoospore release and seasonality of reproduction in *Ecklonia maxima* (Alariaceae, Laminariales). *Br Phycol J* 22:209–214
- Kain JM (1989) The seasons in the subtidal. *Br Phycol J* 24:203–215
- Kawamata S (2001) Adaptive mechanical tolerance and dislodgement velocity of the kelp *Laminaria japonica* in wave-induced water motion. *Mar Ecol Prog Ser* 211:89–104
- Kooijman SALM (2000) Dynamic energy and mass budgets in biological systems, 2nd edn. Cambridge University Press, Cambridge
- Lobban CS, Harrison PJ (1994) Seaweed ecology and physiology. Cambridge University Press, Cambridge
- Lüning K (1979) Growth strategies of three *Laminaria* species (phaeophyceae) inhabiting different depth zones in the sublittoral region of Helgoland (North Sea). *Mar Ecol Prog Ser* 1:195–207
- Lüning K (1990) Seaweeds: their environment, biogeography, and ecophysiology. Wiley, New York
- Lüning K (1993) Environmental and internal control of seasonal growth in seaweeds. *Hydrobiologia* 260/261:1–14
- Lüning K, Dring MJ (1985) Action spectra and spectral quantum yield of photosynthesis in marine macroalgae with thin and thick thalli. *Mar Biol* 87:119–129
- Mann KH (2000) Ecology of coastal waters. With implications for management. Blackwell Science, Oxford
- Martinez LA, Buschmann AH (1996) Agar yield and quality of *Gracilaria chilensis* (Gigartinales, Rhodophyta) in tank culture using fish effluents. *Hydrobiologia* 326/327:341–345
- Martins I, Lopes RJ, Lillebø AI, Neto JM, Pardal MA, Ferreira JG, Marques JC (2007) Significant variations in the productivity of green macroalgae in a mesotidal estuary: implications to the nutrient loading of the system and the adjacent coastal area. *Mar Pollut Bull* 54:678–690
- McDevit DC, Saunders GW (2010) A DNA barcode examination of the laminariaceae (phaeophyceae) in Canada reveals novel biogeographical and evolutionary insights. *Phycologia* 49:235–248
- Neish AC, Shacklock PF, Fox CH, Simpson FJ (1977) The cultivation of *Chondrus crispus*. Factors affecting growth under greenhouse conditions. *Can J Bot* 55:2263–71
- Olsen LM, Holmer M, Olsen Y (2008) Perspectives of nutrient emission from fish aquaculture in coastal waters. Final report, The Fishery and Aquaculture Industry Research Fund
- Petrell RJ, Alie SY (1996) Integrated cultivation of salmonids and seaweeds in open systems. *Hydrobiologia* 326/327:67–73
- Petrell RJ, Tabrizi KM, Harrison PJ, Druehl LD (1993) Mathematical model of *Laminaria* production near at British Columbian salmon sea cage farm. *J Appl Phycol* 5:1–14
- Platt T, Gallegos CL, Harrison WG (1980) Photoinhibition of photosynthesis in natural assemblages of marine phytoplankton. *J Mar Res* 38:687–701
- Rueness J, Fredriksen S (1991) An assessment of possible pollution effects on benthic algae of the outer Oslofjord, Norway. *Oebelia* 17(suppl.):223–235
- Sakshaug E, Johnsen G, Kovacs K (eds) (2009) Ecosystem Barents Sea. Academic, Tapir
- Sanderson JC (2009) Bioremediation using seaweed culture. VDM Verlag Dr. Müller, Düsseldorf
- Schaffelke B (1995) Storage carbohydrates and abscisic acid contents in *Laminaria hyperborea*. *Eur J Phycol* 30:313–317
- Schaffelke B, Lüning K (1994) A circannual rhythm controls seasonal growth in the kelps *Laminaria hyperborea* and *L. digitata* from Helgoland (north sea). *Eur J Phycol* 29:49–56
- Sjøtun K (1993) Seasonal Lamina Growth in two Age groups of *Laminaria saccharina* (L.) Lamour. in Western Norway. *Botanica Marina* 36:433–441
- Sjøtun K (1995) Adaptive aspects of growth and reproduction in two north atlantic *Laminaria* species. Ph.D. thesis, University of Bergen
- Sjøtun K, Gunnarsson K (1995) Seasonal growth pattern of an Icelandic *Laminaria* population (section Simplicis, Laminariaceae, Phaeophyta) containing solid- and hollow-stiped plants. *Eur J Phycol* 30:281–287
- Sjøtun K, Fredriksen S, Rueness J (1996) Seasonal growth and carbon and nitrogen content in canopy and first-year plants of *Laminaria hyperborea* (laminariales, phaeophyceae). *Phycologia* 35:1–8
- Solidoro C, Pecelik G, Pastres R, Franco D, Dejak C (1997) Modelling macroalgae *Ulva rigida* in the Venice lagoon: model structure identification and first parameters estimation. *Ecol Model* 94:191–206
- Stevens C, Hurd C, Isachsen PE (2003) Modelling of diffusion boundary-layers in subtidal macroalgal canopies: the response to waves and currents. *Aquat Sci* 65:81–91
- Subandar A, Petrell RJ, Harrison PJ (1993) *Laminaria* culture for reduction of dissolved inorganic nitrogen in salmon farm effluent. *J Appl Phycol* 5:455–463
- Sundene O (1953) The algal vegetation of Oslofjord. Skrifter utgitt av Det Norske Vitenskaps-Akademi i Oslo. I Matematisk-naturvidenskapelig klasse, Det Norske Vitenskaps-Akademi
- Trancoso AR, Saraiva S, Fernandes L, Nina P, Leitao P, Neves R (2005) Modelling macroalgae using a 3D hydrodynamic-ecological model in a shallow, temperate estuary. *Ecol Model* 187:232–246
- Troell M, Joyce A, Chopin T, Neori A, Buschmann AH, Fang JG (2009) Ecological engineering in aquaculture—potential for integrated multi-trophic aquaculture (IMTA) in marine offshore systems. *Aquaculture* 297:1–9
- Wassmann P, Slagstad D, Riser CW, Reigstad M (2006) Modelling the ecosystem dynamics of the Barents Sea including the marginal ice zone II. Carbon flux and interannual variability. *J Mar Syst* 59:1–24